Water vapor profiling techniques (Raman-DIAL) and applications

Prof. Paolo Di Girolamo, Scuola di Ingegneria, Università degli Studi della Basilicata, Italy

- Why are water vapour profiles needed?
- Why are water vapour profiles difficult to measure?
- Observational requirements
- Advantages/disadvantages of lidar vs. passive sensors in water vapou profiling
- Atmospheric scattering phenomena, with their cross-sections and transition life times
- Roto-vibrational Raman scattering effect
- Water vapor profile measurements based on the Raman lidar technique
- Measurement uncertainty and examples of applications
- Water vapor profile measurements based on the differential absorption lidar technique
- Measurement uncertainty and examples of applications

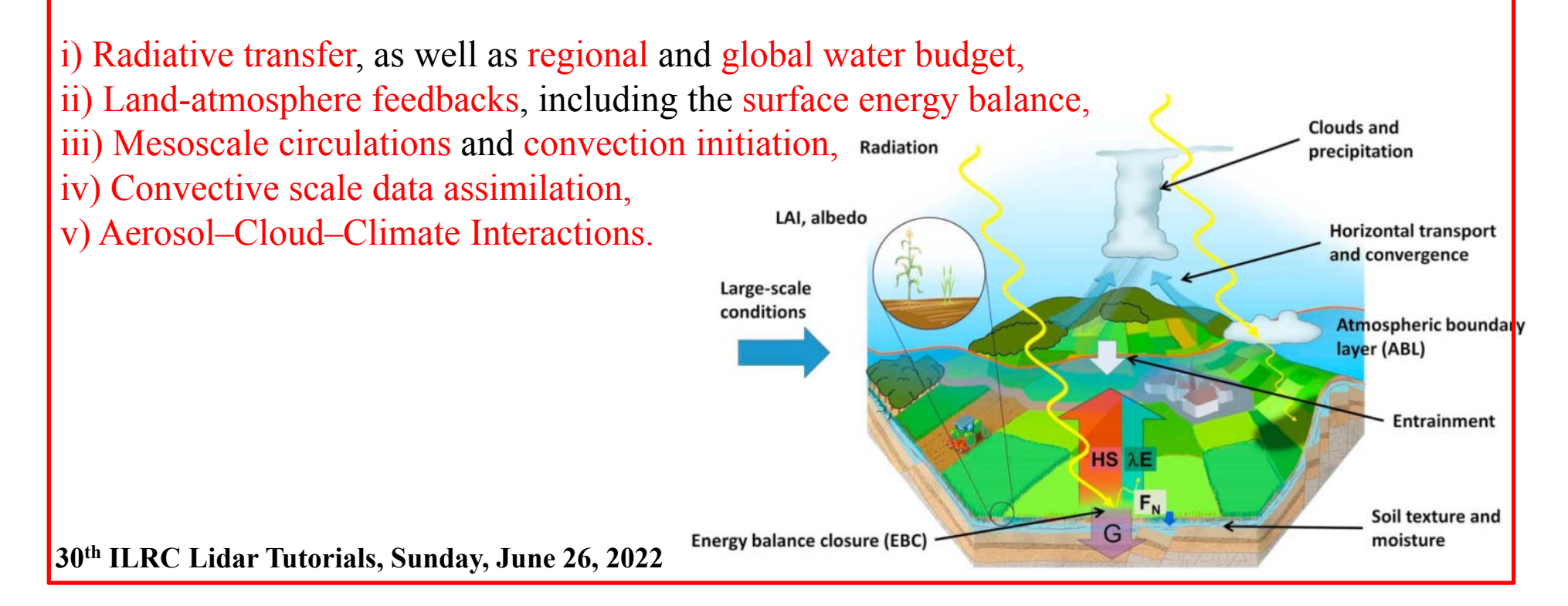
Lidar Tutorials are aimed at researchers who are new to lidar or are early in their lidar careers.

30th ILRC Lidar Tutorials, Sunday, June 26, 2022

Why are water vapour profiles needed?

- An in-depth understanding and advanced prediction of the atmospheric water vapour fields is fundamental for a sustainable development of the Earth system.
- Our understanding of the water cycle still shows critical gaps on all temporal and spatial scales, mainly due to a lack of accurate high vertical resolution measurements of water vapour profiles with high temporal-horizontal resolution, especially in the lower troposphere.
- Accurate, high space and time resolution water vapour profile observations in the lower troposphere are essential for improving weather forecasting and re-analyses.

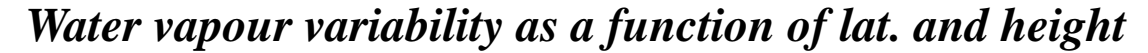
Global scale measurements of 3-dimensional water vapour profiles would have a strong impact on our system understanding in four key research areas:

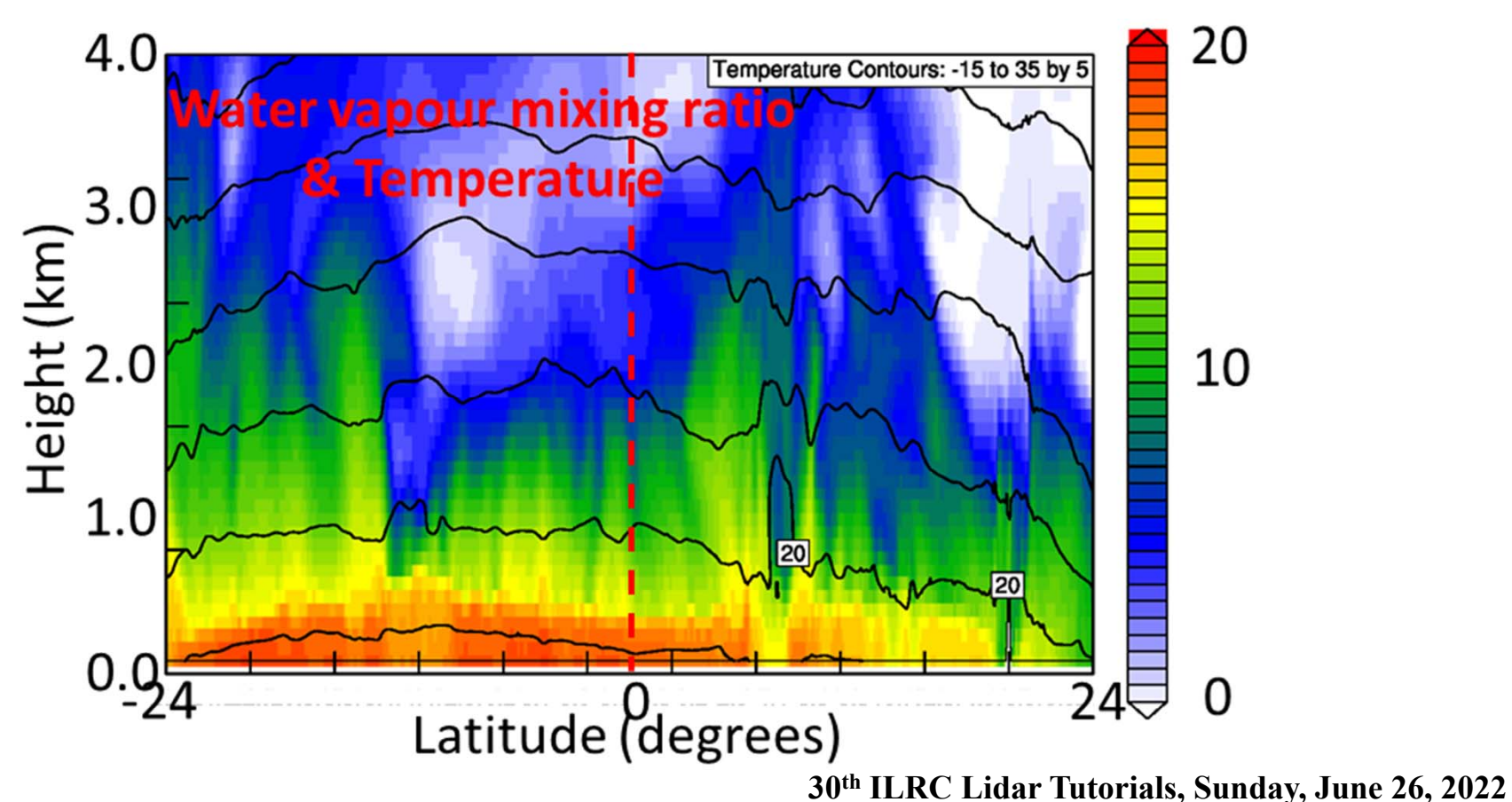


Why are water vapour profiles difficult to measure?

Vertical humidity and temperature profiles show a high space-time variability, with a mutual non-linear dependence mainly associated with their link within the Clausius-Clapeyron equation.

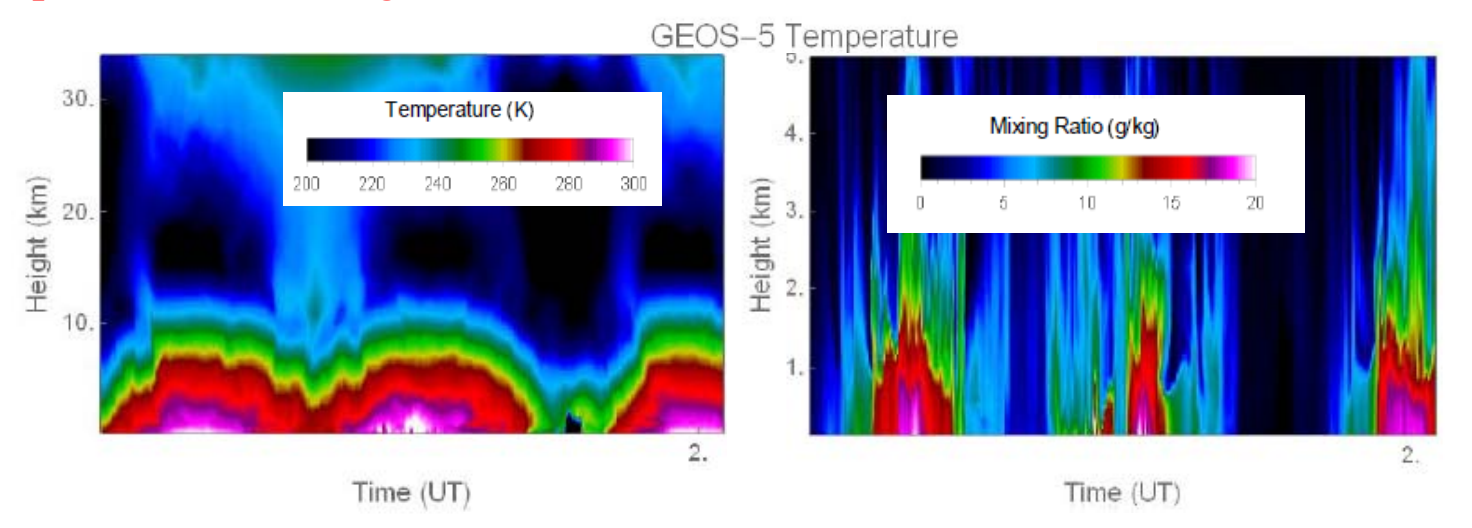
This strong non-linear coupling causes the high space-time variability observed in the temperature profiles in the different climatic regions to translate into a strong space-time variability of the humidity profiles.





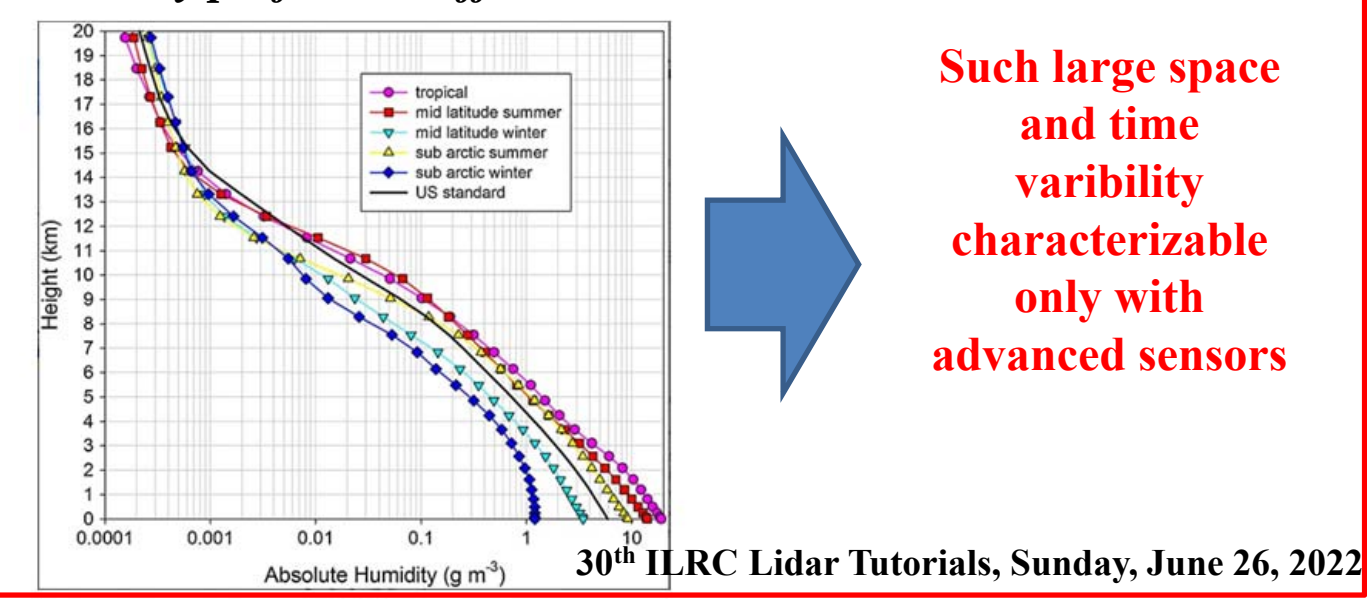
Why are water vapour profiles difficult to measure?

Specifically, the atmospheric humidity at surface level varies by over an order of magnitude between tropical and arctic regions.



Abs. humidity decreases with height by 5 orders of magnitude, especially in tropical regions.

Absolute humidity profiles in different climatic zones



Observational requirements

Observational requirements to be fulfilled in terms of water vapour mixing ratio measurements by networks of remote sensors (satellite and ground-based) can be identified considering four primary application fields:

- (1) Monitoring,
- (2) Verification and calibration,
- (3) Data assimilation,
- (4) Process studies.

For the purpose of assessing climate trends, accurate water vapour measurements are needed not only at the Earth's surface, but also throughout the entire troposphere and stratosphere.

profile observational vapour requirements considering the above Reviews of Geophysics four primary application fields was carried out by Wulfmeyer et al. (2015)





REVIEW ARTICLE

- · Huge observational gaps exist in lower tropospheric thermodynamic profiling
- . Closing these gaps is essential for progress in weather and dimate research.
- · Ground-based passive and active remote sensing systems can dose

Correspondence to: V. Wulfmeyer,

volker.wulfmeves@uni-hohenheim.de

Citation

Wulfmeyer, V., R. M. Hardesty, D. D. Turner, A.Behrendt, M. P. Cadeddu, P. Di Girolamo. P. Schlüssel, J. Van Baelen, and F. Zus (2015), A review of the remote sensing of lower tropospheric thermodynamic profiles and its indispensable role for the understanding and the simulation of water and energy cycles, Rev. Geophys., 53.819-895. doi:10.1002/2014RG000476.

A review of the remote sensing of lower tropospheric thermodynamic profiles and its indispensable role for the understanding and the simulation of water and energy cycles

Volker Wulfmeyer¹, R. Michael Hardesty², David D. Turner³, Andreas Behrendt¹, Maria P. Cadeddu⁴, Paolo Di Girolamo⁵, Peter Schlüssel⁶, Joël Van Baelen⁷, and Florian Zus⁸

1 Institute of Physics and Meteorology, University of Hohenheim, Stuttgart, Germany, 2 Cooperative Institute for Research in Environmental Sciences, University of Colorado, Boulder, Colorado, USA, 3National Severe Storms Laboratory, National Oceanic and Atmospheric Administration, Norman, Oklahoma, USA, Environmental Science Division, Argonne National Laboratory, Argonne, Illinois, USA, Scuola di Ingegneria, Università degli Studi della Basilicata, Potenza, Italy, Luropean Organisation for the Exploitation of Meteorological Satel lites, Darmstadt, Germany, Laboratoire de Météorologie Physique, Observatoire de Physique du Globe de Clermont-Ferrand, Aubiere, France, ⁸German Research Center for Geosciences, Potsdam, Germany

Abstract A review of remote sensing technology for lower tropospheric the modynamic (TD) profiling is presented with focus on high accuracy and high temporal-vertical resolution. The contributions of these instruments to the understanding of the Earth system are assessed with respect to radiative transfer, land surface-atmosphere feedback, convection initiation, and data assimilation. We demonstrate that for progress in weather and climate research, TD profilers are essential. These observational systems must resolve gradients of humidity and temperature in the stable or unstable atmospheric surface layer dose to the ground, in the mixed layer, in the interfacial layer—usually characterized by an inversion—and the lower

Observational Requirements

Observational systems must resolve humidity gradients in the:

- stable and unstable atmospheric surface layer close to the ground,
- mixed layer,
- interfacial layer,
- lower troposphere.

| Parameter | Monitoring | Verification | Data Assimilation | Process Studies |
|-----------------------------|------------|-----------------|--------------------------|------------------------|
| Vert. resolution in ABL (m) | | | | |
| Surface layer | 10–30 | 10–30 | 10–30 | 10 |
| Mixed layer | 100–300 | 100–300 | 100–300 | 10–100 |
| Interfacial layer | 10–100 | 10–100 | 100 | 10–100 |
| Lower free troposphere | 300–500 | 300–500 | 300–500 | 100 |
| Time resolution (min) | <60 | <15 | 5–15 | 1/60 to 1 |
| WV noise error (%) | <10 | <5 | <10 | <10 |
| WV bias (%) | 2–5 | 2–5 | <5 | <5 |
| T noise error (K) | 1 | 1 | 1 | 0.5 |
| T bias (K) | 0.2-0.5 | 0.2-0.5 | 0.2-0.5 | 0.2-0.5 |
| Coverage | All | climate regions | | - |

Observational requirements

The observational requirements for atmospheric water vapour measurements in terms of vertical resolution and accuracy are similar in the different application fields.

In particualr, a vertical resolution of 10-100 m is required to revolse the moisture gradients in the lower troposphere.

In each single vertical range bin, the systematic uncertainty (or bias) affecting water vapour mixing ratio measurements should not exceed 5 %, while the random uncertainty should be smaller than 10 %.

Regarding the temporal resolution, the observational requirements are different in the different applications. For example, in process studies and in the characterization of turbulent flows, high resolutions are required, typically between 1 and 60 seconds, while in data assimilation for forecasting purposes and in the verification and calibration of sensors and models, the requirements in terms of temporal resolution they are milder, typically between 5 and 15 minutes.

Similar requirements were obtained by the World Meteorological Organization (Integrated Global Observing Systems), the World Climate Research Program (WCRP) and the Global Climate Observing System (GCOS).

Advantages/disadvantages of lidar vs. passive sensors in water vapour profiling

These requirements cannot be met with passive remote sensing techniques (neither in the infrared nor in the microwave region) so that the lower troposphere remains an under-characterized portion of the atmosphere in terms of water vapour and temperature fields.

Raman lidars and DIALs can carry out measurements with a range resolution of a few 10 m to several 100 m and a temporal resolution of 1 s to several 10 min.

However, lidar systems are more complex in terms of system setup, maintenance, and routine operation, involving components such as the laser transmitter, the receiver, and the data acquisition system.

Lidar systems typically carry out measurements with high SNRs in cloud-free atmospheres and cloudy atmospheres through optically thin clouds (τ <0.3).

In the presence of **optically thick clouds**, range-resolved measurements are possible:

- within clouds for an optical thickness typically not exceeding 2;
- otherwise, up to the cloud base or shortly within

Measurements during rain are hardly possible due to the large extinction of the transmitted laser radiation.

Atmospheric scattering phenomena, with their cross-sections and transition life times

| Scattering process | Frequency | Cross-section (cm ² sr ⁻¹) | Transition life time (sec) |
|---------------------------|----------------|---------------------------------------------------|----------------------------|
| Rayleigh scattering | $v_r = v_0$ | 10-27 | < 10-14 |
| Mie scattering | $v_r = v_0$ | 10-8-10-27 | < 10 ⁻¹⁴ |
| Ordinary Raman scattering | $v_r \neq v_0$ | 10-30 | < 10 ⁻¹⁴ |
| Resonant Raman scattering | $v_r = v_0$ | 10-23 | 10-8-10-14 |
| Fluorescence | $v_r \neq v_0$ | 10-27 | 10-8-10-1 |

Single-scattering monostatic lidar equation:

$$P_{\lambda}(z) = P_0 \, \Delta z \, k \, \frac{A}{z^2} \, \beta_{\lambda}(z) \, T_{\lambda}(z) \, T_{\lambda_0}(z) \, \frac{\lambda}{hc}$$

 $P_{\lambda}(z)$ = received radiant power at wavelength λ , espressed in terms of number of collected photons, from distance z (altitude if pointiong vertically)

 P_0 = single pulse energy

 Δz = vertical extent of the atmospheric scattering volume,

k = overall transmission-reception efficiency,

A = telescope aperture, h = Planck's constant, c = speed of light

 $\beta_{\lambda}(z)$ = backscattering coefficient at the receiving wavelength λ ,

 $T_{\lambda}(z)$ = atmospheric transmissivity at the receiving wavelength λ ,

 $T_{\lambda 0}(z)$ = atmospheric transmissivity at the laser wavelength λ_0 .

Transmissivity terms

The transmissivity terms account for the attenuation of the laser beam as it propagates through the atmosphere:

 $T_{\lambda 0}(z)$ refers to the atmospheric transmissivity from the transmitter to the scattering volume $T_{\lambda}(z)$ refers to the atmospheric transmissivity from the scattering volume back to the receiver

The transmissivity term can be expressed in the following form:

$$T_{\lambda}(z) = \exp -\int_{0}^{z} \left[\alpha_{M}(\xi) + \alpha_{A}(\xi) + \alpha_{AN}(\xi) + \alpha_{sp}(\xi) \right] d\xi$$

where:

- $\alpha_M(z)$ is the extinction coefficient due to the ambient gas molecules,
- $\alpha_A(z)$ is the extinction coefficient due to aerosols,
- $\alpha_{AN}(z)$ is the extinction coefficient due to inelastic scattering phenomena,
- $\alpha_{sp}(z)$ is the absorption coefficient due to the atomic or molecular gaseous species, if any, with an absorption line or band at wavelength λ .

Roto-vibrational Raman scattering

Atmospheric molecules scatter the incident electromagnetic radiation not only at the laser wavelength, but also at specific shifted wavelengths due to the Raman effect.

As a result of the roto-vibrational Raman scattering effect, each molecular species is characterized by a specific frequency shift v_s , such that if v_0 is the laser frequency, the shifted frequency at which the Raman scattering phenomenon is observed is v_r :

$$v_r = v_0 \pm v_S$$

$$\lambda_r = c/(v_0 \pm v_S)$$

Each gaseous species has its own characteristic Raman frequency shift v_s .

The roto-vibrational Raman shifts (expressed in wave numbers) of the most important atmospheric species are:

| O_2 | 1556 cm ⁻¹ |
|--------------------------|-----------------------|
| N_2^2 | 2331 cm ⁻¹ |
| H_2O | 3652 cm ⁻¹ |
| $\overline{\text{CO}}_2$ | 1286 cm ⁻¹ |
| SO_2 | 1151 cm ⁻¹ |

Roto-vibrational Raman scattering

In the Raman lidar technique, the receiver is tuned on the Raman shifted wavelengths of the atmospheric species of interest.

Based on the single-scattering monostatic lidar equation, properly modified, the intensity of the Raman scattering echoes from any particular atmospheric species are proportional to the concentration of the species:

$$P_{\lambda_{sp}}(z) = P_0 \Delta z k \frac{A}{z^2} n_{sp}(z) \sigma_{sp} T_{\lambda_{sp}}(z) T_{\lambda_0}(z) \frac{\lambda}{hc}$$

where:

- $n_{sp}(z)$ = number density of the species of interest,
- σ_{sp} = its Raman cross section,
- $T_{\lambda sp}(z)$ = atmospheric transmissivity at the Raman shifted wavelength λ_{sp} ,
- $T_{\lambda 0}(z)$ = atmospheric transmissivity at the laser wavelength λ_0 .

Advantages and disadvantages of the Raman lidar technique Advantages

- The possibility to profile several atmospheric species based on the transmission of a single laser wavelength.
- The laser wavelength can be anyone, as long as within an atmospheric window (near ultraviolet and visible).
- Similarly to the Rayleigh cross section, the Raman cross section has a wavelength dependence as λ^{-4} and lasers operating in the ultraviolet region are therefore preferable.

Disadvantages

The major disadvantage of this technique is represented by the limited Raman scattering cross -section (10⁻³⁰ cm² sr⁻¹ against 10⁻²⁷ cm² sr⁻¹ of Rayleigh scattering).

The technique is therefore limited to applications where the investigated atmospheric species are present in sufficiently high concentrations.

Lidar Raman is successfully used to profile water vapor, SO₂, CO₂ and CH₄.

Due to the small Raman cross section, the Raman technique applied to water vapour profiling requires the use of high power laser sources (typically 5-10 W) and large-aperture telescopes (typically 30-50 cm diamater primary mirrors).

The application of the Raman technique to water vapour profiling is more effective at night, with daytime measurements degraded by solar background noise.

Daytime applications may involve the use of laser sources operating in the "solar blind" spectral region, where solar radiance produces a very small noise, comparable with the intrinsic noise of detectors). 240 to 280 nm are completely absorbed by the ozone layer

Water vapor profile measurements based on the Raman lidar technique

• Water vapor mixing ratio profile measurements based on the Raman lidar technique rely on the simultaneous measurement of the roto-vibrational Raman backscattered echoes from water vapour and molecular nitrogen, $P_{\lambda_{N_2}}(z)$ and $P_{\lambda_{H_2O}}(z)$ respectively, which are given by the expressions:

$$P_{\lambda_{H_2O}}(z) = P_0 \frac{c\tau}{2} k'' \frac{A}{z^2} n_{H_2O}(z) \sigma_{H_2O} T_{\lambda_{H_2O}}(z) T_{\lambda_0}(z) \frac{\lambda}{hc}$$

$$P_{\lambda_{N_2}}(z) = P_0 \frac{c\tau}{2} k' \frac{A}{z^2} n_{N_2}(z) \sigma_{N_2} T_{\lambda_{N_2}}(z) T_{\lambda_0}(z) \frac{\lambda}{hc}$$

where:

- σ_{N2} and σ_{H2O} represent the Raman cross section of N_2 and water vapor, respectively,
- $n_{N2}(z)$ and $n_{H2O}(z)$ their numerical densities.

The factors k' and k" are the overall optical efficiencies for the two measurement channels.



The overall optical efficiencies include a transmission term and a reception term.

The transmission term is the same for the two channels, while the reception terms of the two channels, associated with the different devices in the two channels (dichroic beam-splitters, interference filters, etc. and the quantum efficiency of the used detectors) are different.

Water vapor profile measurements based on the Raman lidar technique

The intensity of the two roto-vibrational Raman lidar echoes is proportional to the concentration of the two species

Consequently the ratio of the two roto-vibrational Raman lidar echoes is proportional to the water vapor mixing ratio $x_{H2O}(z)$ (expressed in volumetric units), which is defined as the ratio of the water vapor number density $n_{H2O}(z)$ over the ambient gas number density n(z):

$$x_{H_2O}(z) = \frac{n_{H_2O}(z)}{n(z)}$$

- N_2 is a well mixed species in the atmosphere up to ~100 km
- its mixing ratio is constant and equal to 0.78.



Thus,
$$n_{N2}(z) = 0.78 \text{ n } (z)$$

Therefore:

$$x_{H_2O}(z) = 0.78 \frac{P_{\lambda_{H_2O}}(z)}{P_{\lambda_{N_2}}(z)} \frac{k'}{k''} \frac{\sigma_{N_2}}{\sigma_{H_2O}} \frac{T_{\lambda_{N_2}}(z)}{T_{\lambda_{H_2O}}(z)}$$

Water vapor profile measurements based on the Raman lidar technique

Water vapour mixing ratio

$$x_{H_2O}(z) = k \frac{P_{H_2O}(z)}{P_{N_2}(z)} \Delta T_{\lambda_{H_2O}, \lambda_{N_2}}$$

 $P_{H_2O}(z)$, $P_{N_2}(z)$ background subtracted water vapour and molecular nitrogen roto-vibrational Raman signal intensities, respectively

k lidar system's calibration coefficient and

differential transmission term, which accounts for the different atmospheric transmission by molecules and aerosols at the two Raman wavelengths λ_{H_2O} and λ_{N_2}

$$k=0.78 \cdot \frac{k'}{k''} \frac{\sigma_{N_2}}{\sigma_{H_2O}}$$

$$\Delta T_{\lambda_{H_{2}O},\lambda_{N_{2}}} = \frac{T_{\lambda_{N_{2}}}(z)}{T_{\lambda_{H_{2}O}}(z)} = \frac{T_{\lambda N2}^{mol}(z)}{T_{\lambda H2O}^{mol}(z)} \frac{T_{\lambda N2}^{aer}}{T_{\lambda H2O}^{aer}(z)}$$

Differential transmission term

If the aerosol load is negligible, the ratio

$$T_{\lambda_{N_2}}(z)$$
 $T_{\lambda_{H_2O}}(z)$

can be exactly determined thorugh the Rayleigh scattering theory from an atmospheric density profile (model atmospheres, radiosondes, other source).

Even in conditions of heavy aerosol load, the ratio can be determined with an uncertainty not exceeding 1-2%, based on the simultaneous aerosol extinction measurements from the same lidar or a nearby one, assuming the aerosol extinction coefficient to scale with the wavelength as $\lambda^{-\delta}$, with $0.5 < \delta < 2$.

Calibration

Calibration of water vapour Raman lidar systems can be carried out based on the comparison with independent profiling sensors performing water vapour mixing ratio measurements:

- Radiosondes launched directly from the lidar site or from a nearby location,
- Microwave radiometers

Calibration

More specifically, a mean calibration coefficient can be estimated by comparing the Raman lidar measurements with the radiosonde profiles over an extended number of cases when data from both systems are simultaneously available.

Typically, in order to properly assess of the mean calibration value, its standard deviation and any possible temporal trend, a number of approximately 50 comparisons covering a variety of weather conditions is desirable).

The standard deviation of the mean calibration coefficient represents the major portion of the systematic uncertainty (or bias) affecting water vapour mixing ratio profile measurements.

In case of field campaigns the constancy of the calibration coefficient should be verified, based on the comparison with radisosondes, at the beginning and end of the measurement period.

When the Raman lidar is located in the proximity of the radiosonde launching facility, the comparisons to estimate the calibration coefficients are typically carried out in the vertical region from the surface up to ~ 2 km.

Within this altitude interval:

- Raman lidar signals are strong and characterized by high signal-to-noise ratios and small statistical fluctuations.
- the horizontal drift of the radiosonde with respect to the vertical of the lidar station is limited, and the two sensors can be actually assumed to be sounding the same air masses.

The water vapor mixing ratio calibration constant k is obtained through a best-fit procedure applied to the Raman lidar and radiosonde data.

Determination of the Raman receiving wavelengths

The determination of the receiving wavelengths relies on the conversion of the laser emission wavelength λ_0 into the frequency domain, considering frequency (Hz) or wavenumber (cm⁻¹) units

Wavenumbers are more frequently considered because spectroscopic Raman shifts of atmospheric molecules are tipically expressed in in wavenumbers.

$$v(cm^{-1}) = 10^7 x \frac{1}{\lambda(nm)}$$

$$\lambda_0 = 354.71 \text{ nm}$$



$$v_0 = 28192 \text{ cm}^{-1}$$

$$\nu_{r}\!\!=\!\!\nu_{0}^{}\pm\nu_{S}^{}$$

| O_2 | 1556 cm ⁻¹ |
|--------------------------|-----------------------|
| N_2^2 | 2331 cm ⁻¹ |
| H_2O | 3652 cm ⁻¹ |
| $\overline{\text{CO}}_2$ | 1286 cm ⁻¹ |
| SO_2 | 1151 cm ⁻¹ |

$$v_r = (28192 - 1556) \text{ cm}^{-1} = 26636 \text{ cm}^{-1}$$
 $v_r = (28192 - 2331 \text{ cm}^{-1} = 25861 \text{ cm}^{-1})$
 $v_r = (28192 - 3652) \text{ cm}^{-1} = 24540 \text{ cm}^{-1}$
 $v_r = (28192 - 1286) \text{ cm}^{-1} = 26906 \text{ cm}^{-1}$
 $v_r = (28192 - 1151) \text{ cm}^{-1} = 27041 \text{ cm}^{-1}$
 $\lambda_r = 375.43 \text{ nm}$
 $\lambda_r = 386.68 \text{ nm}$
 $\lambda_r = 377.50 \text{ nm}$
 $\lambda_r = 371.66 \text{ nm}$
 $\lambda_r = 371.66 \text{ nm}$

Alternatively

The water vapour mixing ratio can be obtained from the the pure-rotational and roto-vibrational Raman backscattered signals through the expression:

$$x_{H_2O}(z) = K \cdot \Delta Trs(z) \cdot \frac{P_{H_2O}(z)}{P_{ref}(z)}$$

 $P_{ref}(z)$ is a temperature-independent reference signal obtained from a linear combination of the two temperature sensitive rotational Raman lidar signals $P_{Lof}(z)$ and $P_{Hi}(z)$, i.e. the low and high rotational quantum number rotational Raman signals.

Uncertainty affecting water vapour Raman lidar measurements

- Error profiles affecting water vapour Raman lidar measurements can be obtained with the application of Poisson statistics to signal photon counts.
- Signal photon counts are directly measured by the photon counting unit.
- "Virtual" counts can also be obtained from the signals measured by analogue modules (Newsom et al., 2009).
- Poisson statistics is applied to individual lidar signals contributing to the measurements
- Then, through error propagation, the overall error affecting water vapour mixing ratio can be computed as:

$$\frac{\Delta x_{\text{H}_2\text{O}}(z)}{x_{\text{H}_2\text{O}}(z)} = \sqrt{\frac{P_{\text{H}_2\text{O}}(z) + \text{bk}_{\text{H}_2\text{O}}}{P_{\text{H}_2\text{O}}^2(z)} + \frac{P_{\text{N}_2}(z) + \text{bk}_{\text{N}_2}}{P_{\text{N}_2}^2(z)}},$$

 bk_{H2O} , bk_{N2} : sky background signal, primarily associated with solar irradiance, collected in the water vapour and molecular nitrogen channels, respectively.

- Relative statistical error, expressed in percentage if multiplied for 100.
- Absolute statistical error can be obtained by multiplying the above expression for $x_{H2O}(z)$.

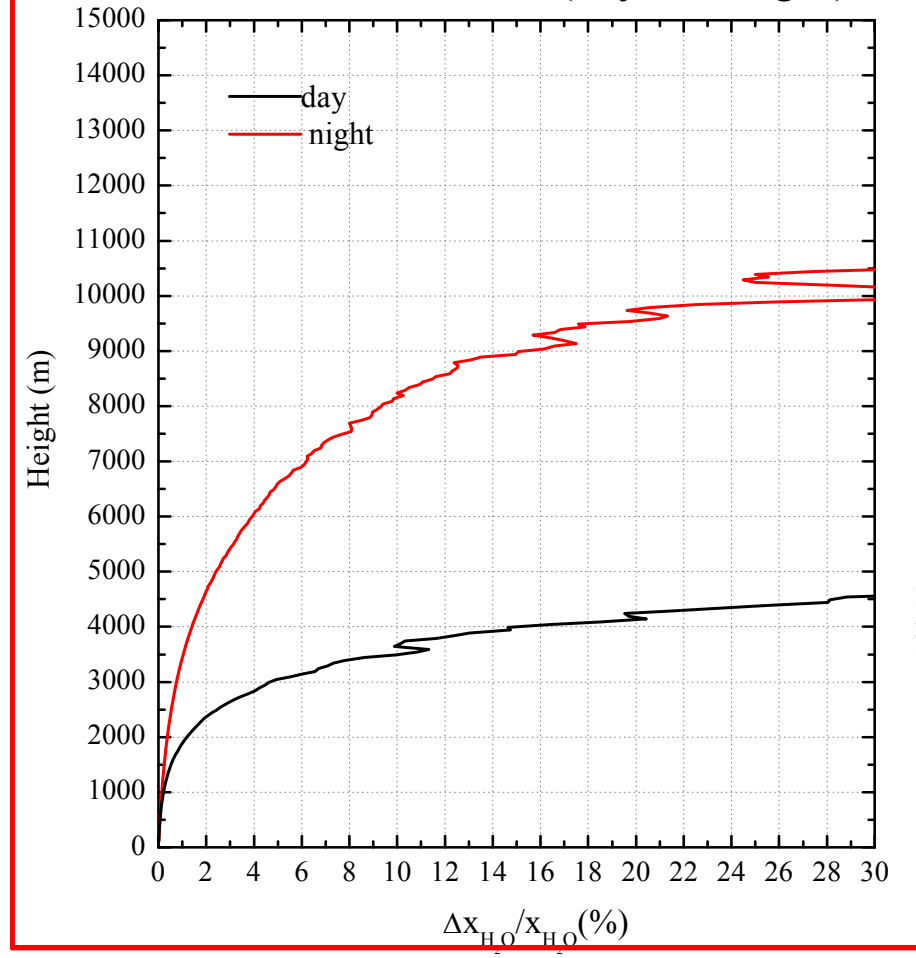
Statistical uncertainty affecting water vapour Raman lidar measurements

Solid state laser source (Nd:; YAG)

- repetition frequency: 100 Hz
- single pulse energy at 354.7 nm: 100 mJ Telescope primary mirror diameter: 0.5 m Time resolution: 1 min (3 hours for CO₂)

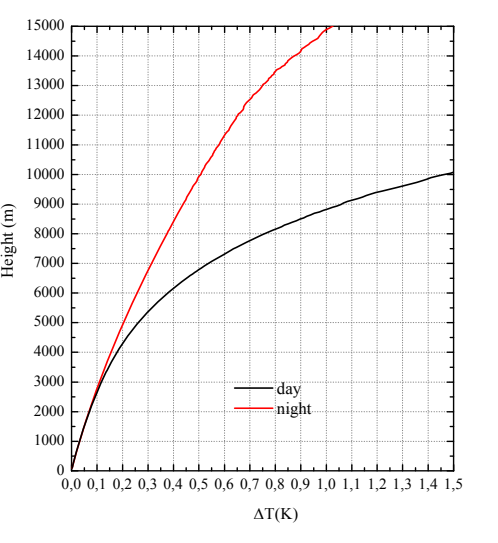
Vertical resolution: 50 m

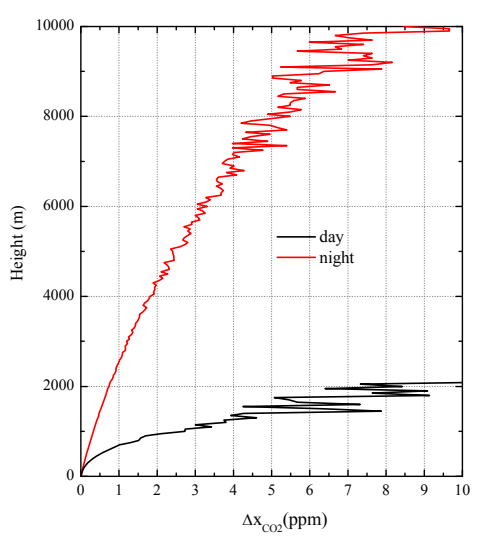
two envir. noise conditions (day and night)



Statistical uncertainty affecting water vapour mixing ratio profile measurements:

- < 5% up to 7 km (night),
- < 20% up to 10 km(night),
- < 10% up to 3.5 km (daytime),
- < 30% up to 5 km (daytime).





Uncertainty affecting water vapour Raman lidar measurements

Poisson statistics accounts for approximately 75% of the total statistical noise affecting water vapour mixing ratio measurement.

The total statistical noise can be estimated through the auto-covariance analysis, while Poisson statistics accounts only for its shot noise contribution, i.e. the contribution associated with the discrete nature of the photons sampled by photon counting devices. Consequently, the application of Poisson statistics to signal photon counts leads to an underestimation of the total statistical noise.

$$\frac{\Delta x_{\rm H_2O}(z)}{x_{\rm H_2O}(z)} \approx \propto \frac{1}{\sqrt{x_{\rm H_2O}(z)}} \frac{1}{\sqrt{A_{\rm tel} E_L v_R \delta t \Delta R}} = \frac{1}{\sqrt{x_{\rm H_2O}(z)}} \frac{1}{\sqrt{A_{\rm tel} P_L \delta t \Delta R}},$$

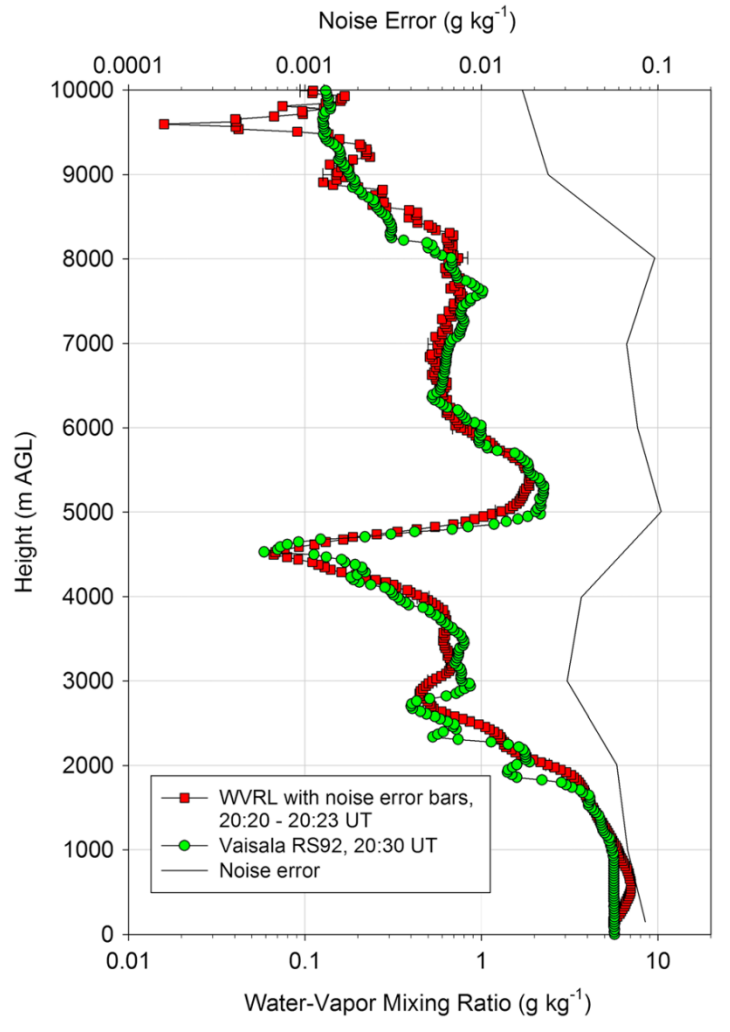
where

- $\Delta x_{\text{H}_2\text{O}}(z)$ is the noise standard deviation of the signal after averaging over a certain number of range bins in the vertical and over a number of shots in time,
- v_R is the repetition rate of the laser transmitter,
- P_L is the laser average power,
- A_{tel} is the telescope area,
- δt is the averaging time,
- $\triangle R$ is the range resolution.

Obviously, under many atmospheric conditions, temporal and spatial resolution can be traded off with respect to the desired precision.

30th ILRC Lidar Tutorials, Sunday, June 26, 2022

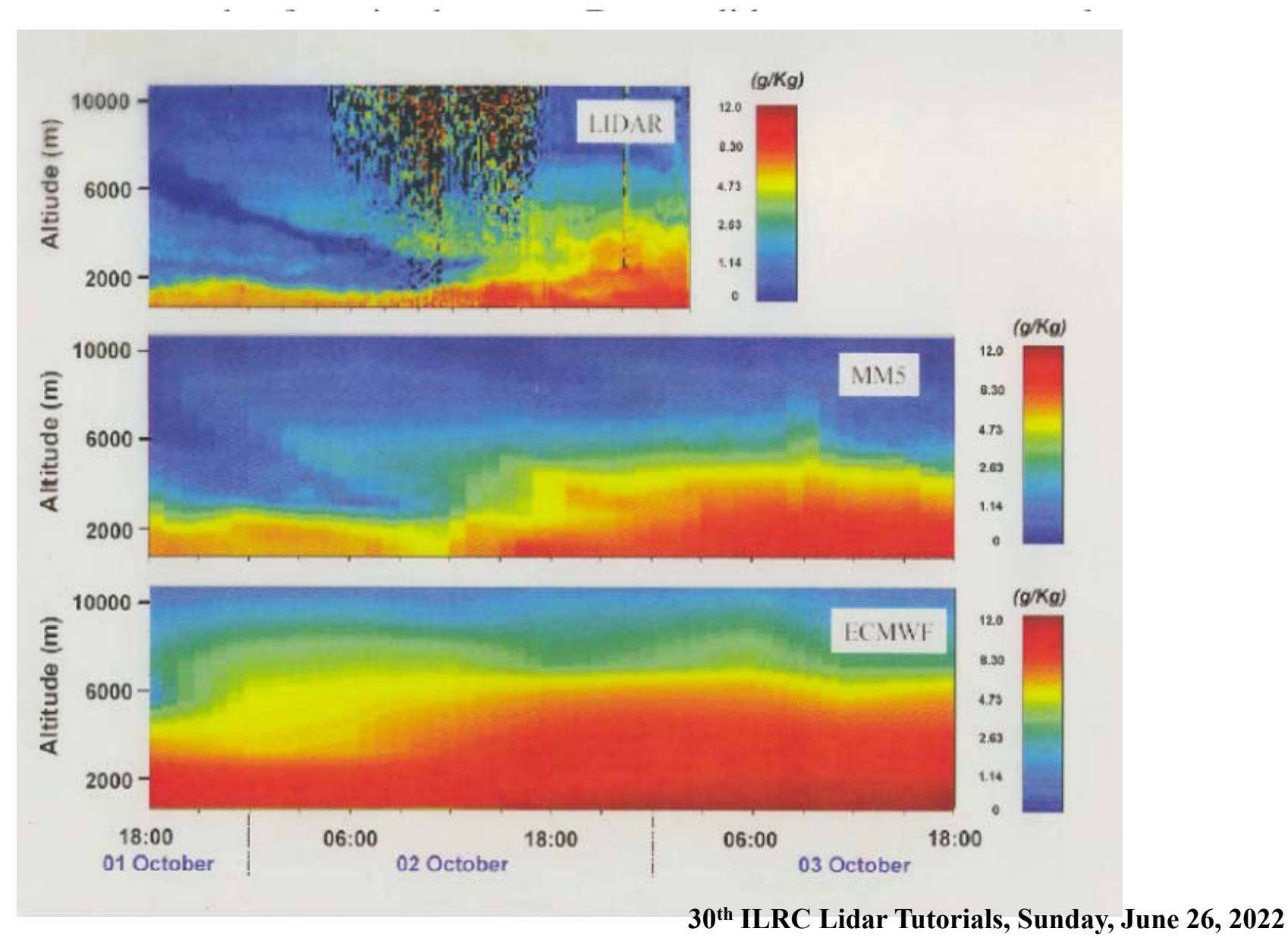
Improved daytime measurement performance have been demonstrated in a variety of papers in the last two decade based on strongly enhenced laser powers and telescope apertures.



Comparison between mixing ratio measurements of the WVRL BASIL (University of Basilicata Raman lidar) and a Vaisala RS92 radiosonde performed on 19 September 2012 at 20:20 UTC. The resolutions of the Raman lidar profile are 3 min and 150 m, respectively. Here BASIL was using 10W power (0.5 J, 20 Hz) of the laser transmitter at 355 nm and a telescope diameter of 0.45 m.

Example of process studies

Dry air stratospheric intrusion episode associated with a tropopause folding event

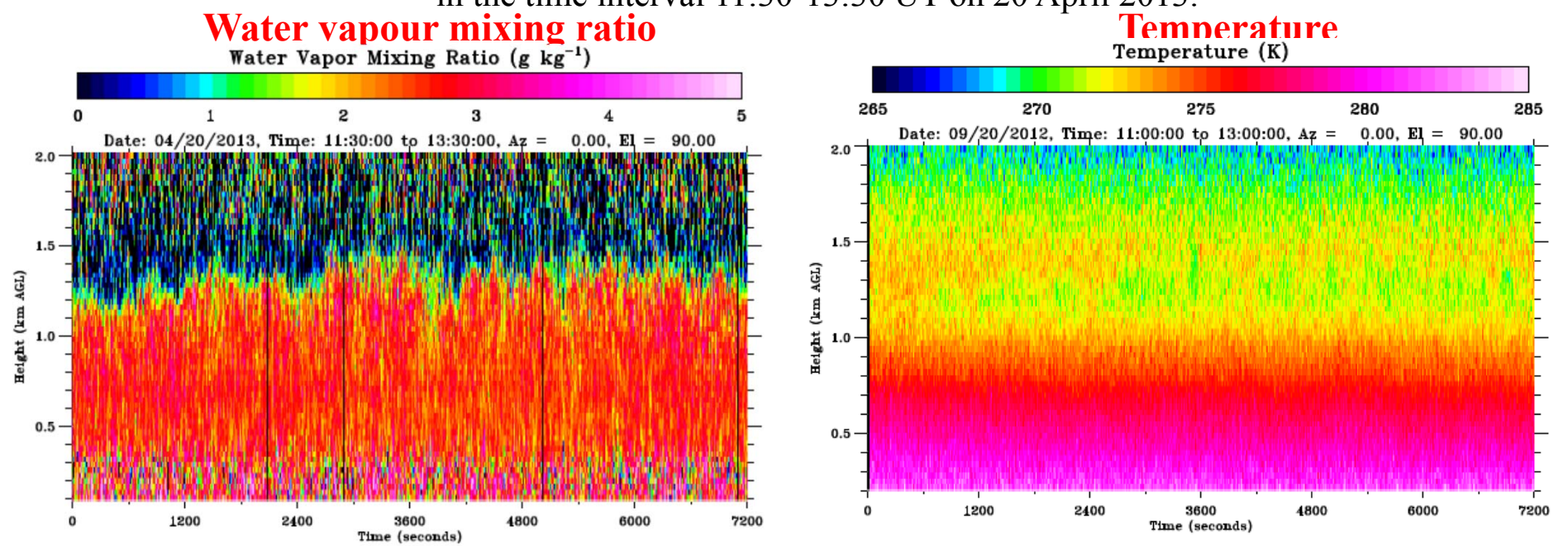


Characterization of Turbulent processes in clear-air conditions

Measurements of the higher-order moments of moisture and temperature fluctuations provide information for the **characterization of turbulent processes** within the Atmospheric Boundary Layer (ABL).

Selection of a 2-h measurement period (11:30-13:30 UT on 20 April 2013) characterized by a uniformly mixed Convective Boundary Layer (CBL).

Time-height cross section of water vapour mixing ratio and temperature in the time interval 11:30-13:30 UT on 20 April 2013.



Variability of water vapour mixing ratio and temperature within the CBL associated with the alternation of updrafts and downdrafts.

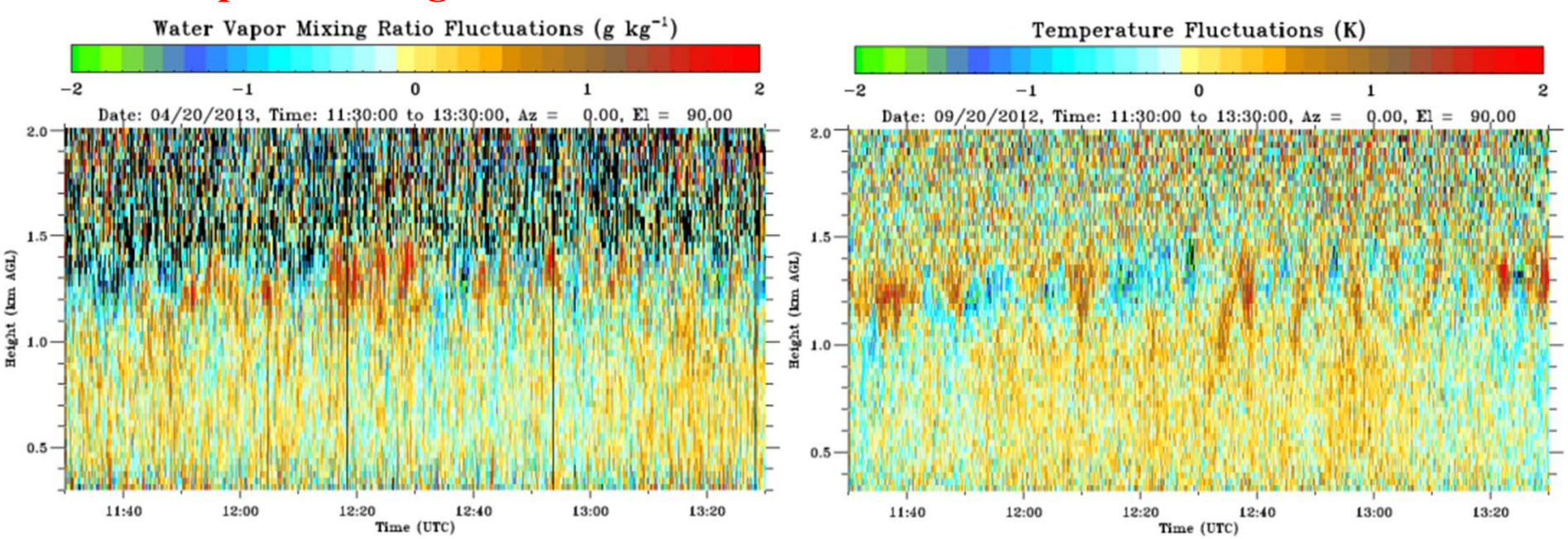
Largest variability of water vapour mixing ratio and temperature observed in the interfacial layer, as a result of the penetration of the warm humid air rising from the ground and the entrainment of cool dry air sinking from the free troposphere

Characterization of Turbulent processes in clear-air conditions

Time-height cross section of water vapour mixing ratio and temperature fluctuations in the time interval 11:30-13:30 UT on 20 April 2013.

water vapour mixing ratio fluctuations

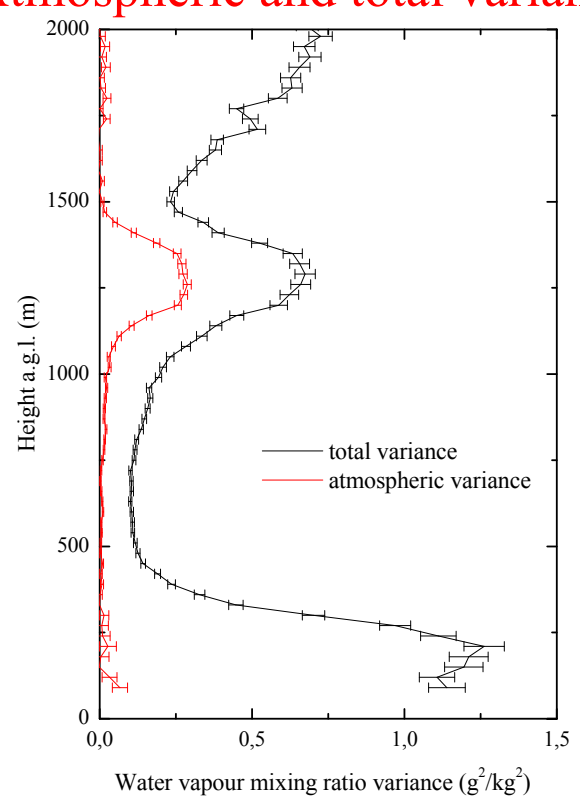
temperature fluctuations

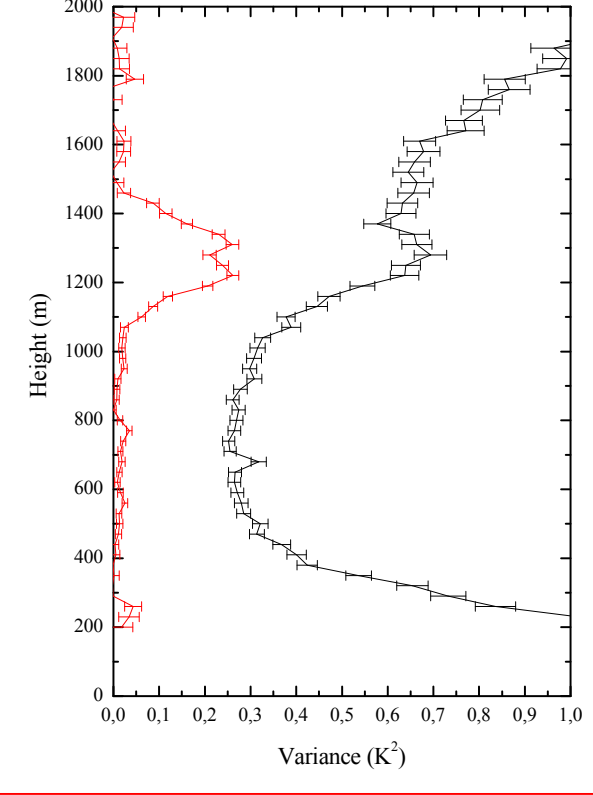


Instantaneous water vapour fluctuations are within \pm 0.5 g/kg in the mixed layer and \pm 1 g/kg in the interfacial layer, while instantaneous temperature fluctuations are within \pm 0.5 K in the mixed layer and \pm 1 K in the interfacial layer.

Characterization of Turbulent processes in clear-air conditions

Atmospheric and total variance for water vapour mixing ratio and temperature





H₂O variance < 0.05 $g^{2/k}g^2$) in the middle and upper portion of the CBL (750 m <z< 1100 m, i.e. 0.6 < z/zi < 0.85) weak surface forcing maximum variance in the interfacial layer: $0.29 \pm 0.032 g^2/kg^2$ at 1260 m.

T variance $< 0.1 \text{ K}^2$ in the middle and upper portion of the CBL up to 1100 (i.e. 0.85 zi).

maximum variance in the interfacial layer: $0.23 \pm 0.03 \text{ K}^2$ at 1310 m

large variability associated with the strong updrafts and downdrafts

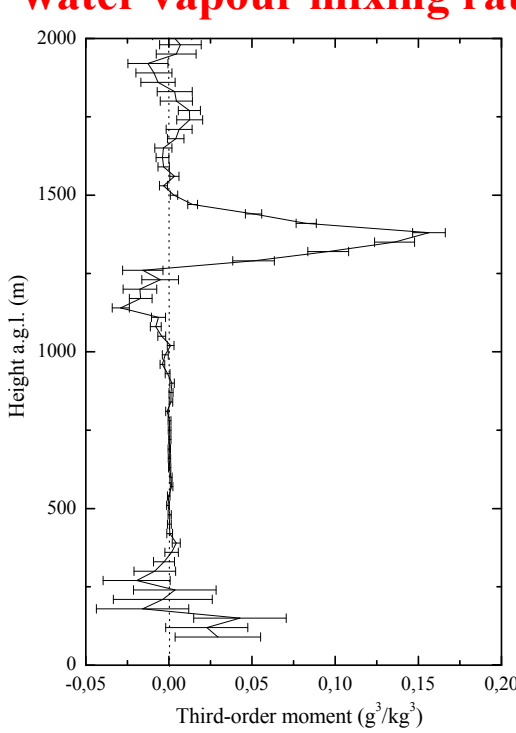
as a result of penetration of warm humid air entrainment of cold dry air sinking from FT

Characterization of Turbulent processes in clear-air conditions

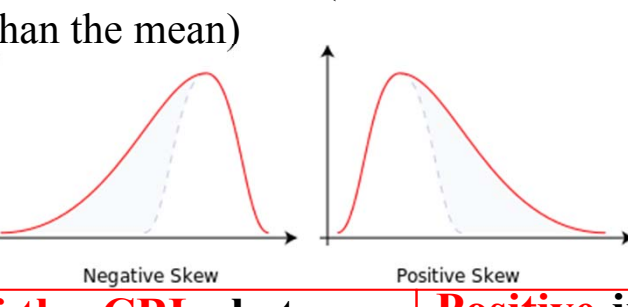
water vapour mixing ratio

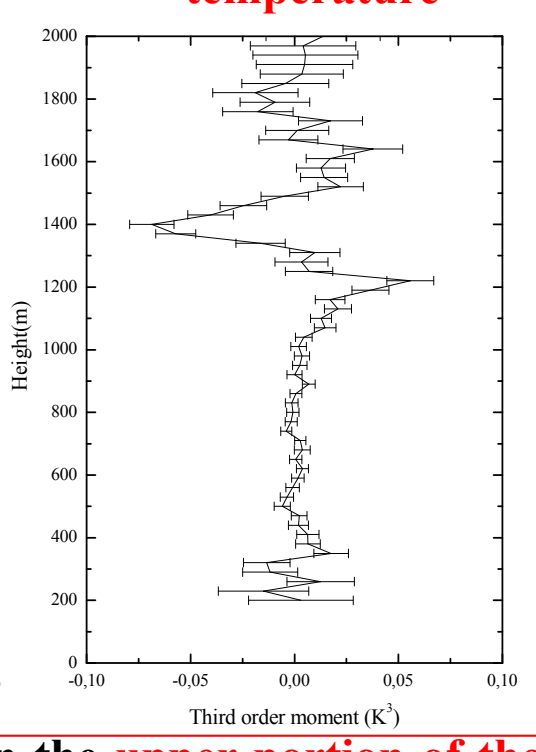
Third-order moment

temperature



The third-order moment quantifies the degree of asymmetry of the distribution of mixing ratio vapour water and temperature fluctuations, with positive values indicating right-skewed a distribution (with the mode smaller than the mean) and negative values indicating a left-skewed distribution (with the mode larger than the mean)





Negative in the upper portion of the CBL, between 900 and 1290 m (0.7 zi < z < zi), with a negative peak value of -0.029 \pm 0.005 g^3/kg^3 at 1140 m.

Entrainment of dry air pockets into the boundary layer, gradually mixing with the environmental air

Positive just above CBL top, with a positive peak of 0.156±0.009 g³/kg³ at 1380 m (z=1.07 zi).

possibly associated with convective plumes that penetrate to this height.

Positive in the upper portion of the CBL, with a positive peak of 0.05 K³ at 1210 m.

Negative just above the CBL top, with a negative peak of -0.08 ± 0.01 K³ at 1400 m).

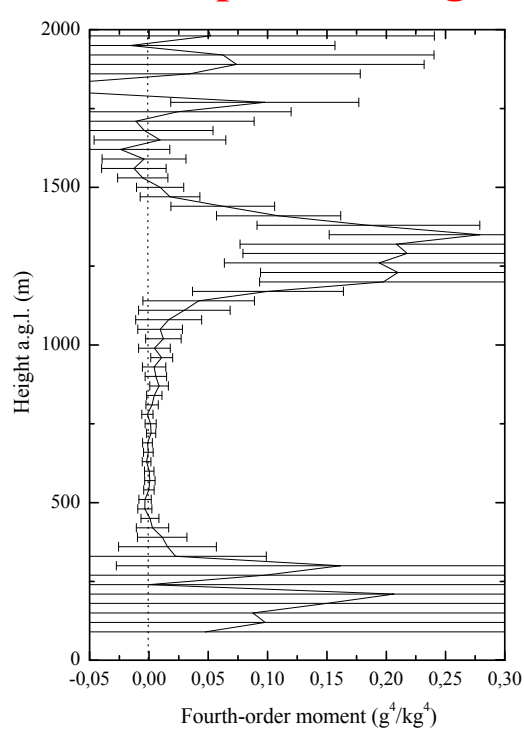
predominant effect of cool air downdrafts above the CBL top associated with thermals of cool air sinking from the free troposphere

Characterization of Turbulent processes in clear-air conditions

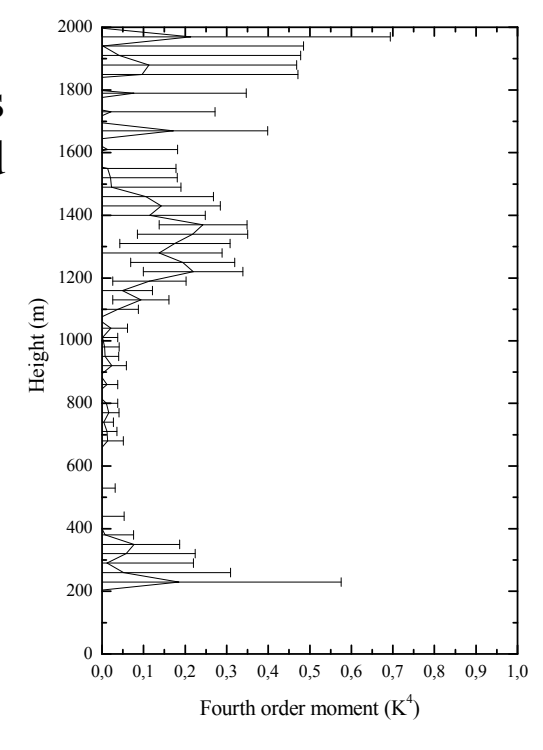
water vapour mixing ratio

Fourth-order moment

temperature



The fourth-order moment quantifies the steepness of the distribution and the width of its peak (peakedness).



Almost zero up to 1100 m

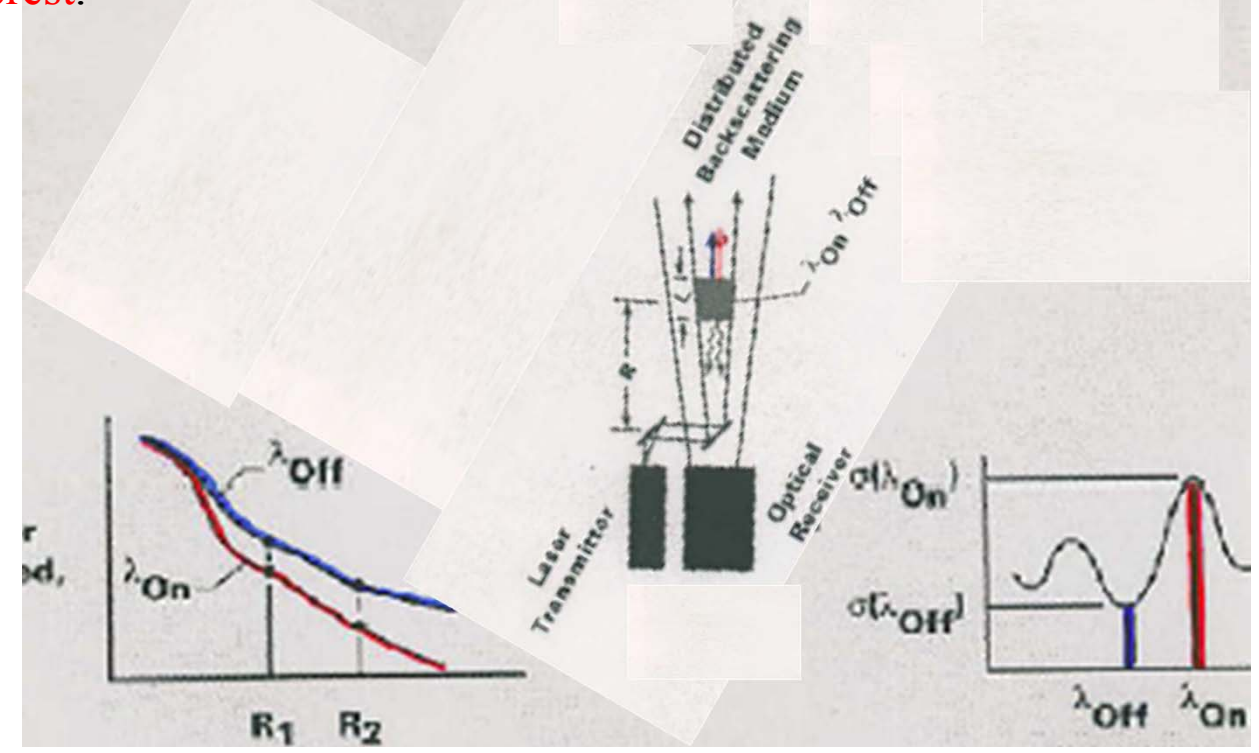
Positive values above 1100 m, reaching a maximum of 0.28 ± 0.13 g⁴/kg⁴ around the top of the CBL (at 1350 m).

Almost zero up to 1100 m **Positive values above 1100 m**, reaching a maximum of $0.23 \pm 0.10 \text{ K}^4$ around the **top of the CBL** (at 1370 m).

Smaller values within the CBL testify moderate quasi-normally distributed humidity and temperature fluctuations, while larger values in the interfacial layer testify stronge fluctuations possibly associated with very vigorous thermals.

- DIAL is an indirect lidar technique based on the measurement of elastic scattering echoes by aerosols and ambient gas, with the species of interest modifying the transmissivity of the laser radiation through the atmosphere.
- The DIAL technique makes use of two laser beams simultaneously transmitted in the atmosphere, one absorbed by the gaseous species of interest (λ_{on}) , while the other, at a slightly shifted wavelength (λ_{off}) , is not absorbed.

• If the two wavelengths are sufficiently close each other, the different intensities of the two elastic echoes $(P_{\lambda on}(z) \text{ and } P_{\lambda off}(z))$ is entirely attributable to the different absorption by the species of interest.



• From the elastic lidar echoes at the two wavelengths it is therefore possible to determine the vertical profile of the absorbing species. The intensities of the two elastic signals, absorbed and non-absorbed, are:

$$P_{\lambda_{on}}(z) = P_0' \frac{c\tau}{2} k' \frac{A}{z^2} \beta_{\lambda_{on}}(z) T_{\lambda_{on}}^2(z) \frac{\lambda}{hc}$$

$$P_{\lambda_{off}}(z) = P_0'' \frac{c\tau}{2} k'' \frac{A}{z^2} \beta_{\lambda_{off}}(z) T_{\lambda_{off}}^2(z) \frac{\lambda}{hc}$$

 P_0 ' and P_0 '' are used to represent the single pulse energy at λ_{on} and λ_{off} , respectively, as in fact single pulse energies of the two distinct emissions can be different.

The transmissivity terms can be written in the form:

$$T_{\lambda_{on}}(z) = \exp \int_{0}^{z} \left[\alpha_{\lambda_{on}}(\xi) + n_{sp}(\xi) \sigma_{\lambda_{on}}^{sp} \right] d\xi$$

$$T_{\lambda_{off}}(z) = \exp \int_{0}^{z} \left[\alpha_{\lambda_{off}}(\xi) + n_{sp}(\xi) \sigma_{\lambda_{off}}^{sp} \right] d\xi$$

where $n_{sp}(z)$ is the number concentration of the absorbing species

 σ_{λ}^{sp} is the absorption cross section of the investyigated species «sp» $\alpha_{\lambda}(z)$ is the extinction coefficient, associated with elastic or inelastic scattering phenomena and with absorption by species different from the investigated one

The ratio of the two signals is equal to:

$$\frac{P_{\lambda_{on}}(z)}{P_{\lambda_{off}}(z)} = \frac{P_0'}{P_0''} \frac{k'}{k''} \frac{\beta_{\lambda_{on}}(z)}{\beta_{\lambda_{off}}(z)} \exp \left\{-2 \int_0^z \left(\alpha_{\lambda_{on}}^s(\xi) - \alpha_{\lambda_{off}}^s(\xi)\right) d\xi\right\} \times \left\{-2 \int_0^z n_{sp}(z) \left(\sigma_{\lambda_{on}}^{sp} - \sigma_{\lambda_{off}}^{sp}\right) d\xi\right\}$$

The logarithm of the ratio of the two signals is equal to:

$$\ln \frac{P_{\lambda_{on}}(z)}{P_{\lambda_{off}}(z)} = \ln \frac{\overline{P_0''}}{P_0'''} \frac{k''}{k'''} + \ln \frac{\overline{\beta_{\lambda_{one}}(z)}}{\overline{\beta_{\lambda_{off}}(z)}} - 2\overline{J}\left(\alpha_{\lambda_{one}}^z(\xi) - \alpha_{\lambda_{off}}^z(\xi)\right) d\xi \qquad - 2\overline{J}n_{sp}(z)\left(\sigma_{\lambda_{one}}^{sp} - \sigma_{\lambda_{off}}^{sp}\right) d\xi$$

If λ_{on} to λ_{off} are sufficiently close each other and are transmitted into the atmosphere almost simultaneously, in the above expression it is possible to consider:

$$\beta_{\lambda on}(z) = \beta_{\lambda off}(z)$$

$$\alpha_{\lambda on}(z) = \alpha_{\lambda off}(z)$$

Thus, we obtain:

$$\left| -\int_{0}^{z} n_{sp}(\xi) \left(\sigma_{\lambda_{on}}^{sp} - \sigma_{\lambda_{off}}^{sp} \right) d\xi = \frac{1}{2} \left[\ln \frac{P_{\lambda_{on}}(z)}{P_{\lambda_{off}}(z)} - \ln \frac{P_{0}'}{P_{0}''} \frac{k''}{k'} \right] \right|$$

Deriving both sides with respect to altitude, the water vapou number density profile of the investigated species "sp" expressed in terms of g/cm³ is obtained.

In the case of water vapour we have:

$$n_{H_2O}(z) = -\frac{1}{2} \frac{1}{\sigma_{\lambda_{on}}^{H_2O} - \sigma_{\lambda_{off}}^{H_2O}} \left\{ \frac{d}{dz} \left[\ln \left(\frac{P_{\lambda_{on}}(z)}{P_{\lambda_{off}}(z)} \right) \right] \right\}$$

where the term $\frac{P_0'}{P_0''}\frac{k''}{k'}$ has disappeared as it is constant with altitude.

The water vapor number density profile is thus easily determinable from the elastic backscatter echoes $P_{\lambda on}(z)$ and $P_{\lambda off}(z)$) if the absorption cross sections are known.

Considering that the system provides measurements with a finite vertical resolution, the DIAL equation get the form:

$$n_{H_2O}(z) = \frac{1}{2 \Delta z} \frac{1}{\sigma_{\lambda_{on}}^{H_2O} - \sigma_{\lambda_{off}}^{H_2O}} \ln \left(\frac{P_{\lambda_{on}}(z + \Delta z) P_{\lambda_{off}}(z)}{P_{\lambda_{off}}(z + \Delta z) P_{\lambda_{on}}(z)} \right)$$

where Δz is the vertical resolution of the measurement.

Advantages and disadvantages of the DIAL technique Advantages

- DIAL systems provide numerous advantages with respect to currently operational water vapour sensors. Among these:
- 1. direct measurement of humidity without any other assumptions;
- 2. day- and night-time operation;
- 3. utilisation of self-calibration nature of the DIAL technique;
- 5. no interference from other trace gases;

Disadvantages

The D.I.A.L. technique, unlike the Raman technique which uses a single laser beam, requires two distinct beams transmitted at two different wavelengths simultaneously into the atmosphere.

The laser source or sources emitting them must be tunable within a certain spectral region to ensure that one of the wavelengths emitted can be tuned on the absorption line or band of the investigated species and of the off-line laser wavelength on the line shoulder.

If a single laser source is available, it must emit two distinct laser pulses at different wavelengths, passing from one wavelength to the other in a very short time compared to the time with which the geophysical phenomena under observation change.

The appropriate application of the dial technique implies a continuous check a continuous check of the on-line laser wavelength tuning on the selected water vapour absorption line and of the off-line laser wavelength on the line shoulder.

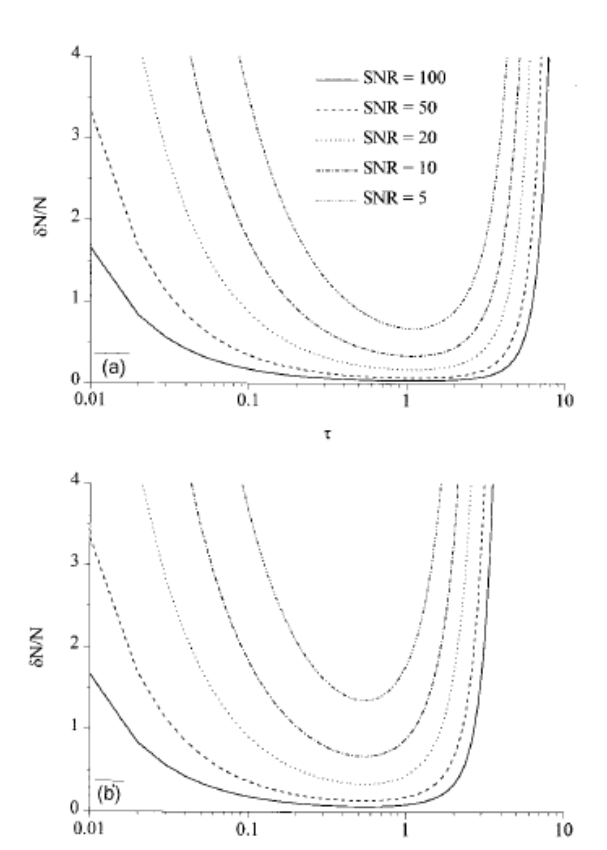
Uncertainty affecting water vapour DIAL measurements

For the shot-noise limited measurements, the error is:

$$rac{\delta N}{N} = rac{K_{\tau}}{ au\sqrt{m_0} \; (\mathrm{SNR})} imes \left\{ rac{\exp(2 au)[1 + \exp(2 au/K_{\tau})]}{2} + 1
ight\}^{1/2}$$

For background or dark-current noise limited measurements, the error is

$$\frac{\delta N}{N} = \frac{K_{\tau}}{\tau \sqrt{m_0} \text{ (SNR)}} \left\{ \frac{\exp(4\tau)(1 + \exp(4\tau/K_{\tau})}{2} + 1 \right\}^{1/2}.$$



 $K\tau$ is the ratio between optical depth τ and range cell differential optical depth $\Delta \tau$, SNR is the signal-to-noise ratio for the power P_{OFF} of the λ_{OFF} return signal,

$$SNR = P_{\lambda off} / \sigma_{\lambda off} = P_{\lambda off} / (P_{\lambda off})^{0.5} = (P_{\lambda off})^{0.5}$$

 m_0 is the total number of laser shots.

For shot-noise-limited measurements, as typically those carried out in the visible and UV at nighttime, the optimum one-way optical depth for the selected line must approximate 1.1, after which the signal becomes too attenuated for accurate measurement.

For background or dark-current noise limited measurements, which correspond to UV-visible daytime and IR measurements, the optimum one-way optical depth for the selected line must approximate 0.55.

30th ILRC Lidar Tutorials, Sunday, June 26, 2022

Uncertainty affecting water vapour DIAL measurements

$$\frac{\sigma_{N_{WV}}}{N_{WV}} \sim \frac{1}{\Delta \tau_{WV}} \frac{1}{\sqrt{A_{tel} P_L \delta t \Delta R}} \sim \frac{1}{\sqrt{A_{tel} P_L \delta t \Delta R^3}}$$

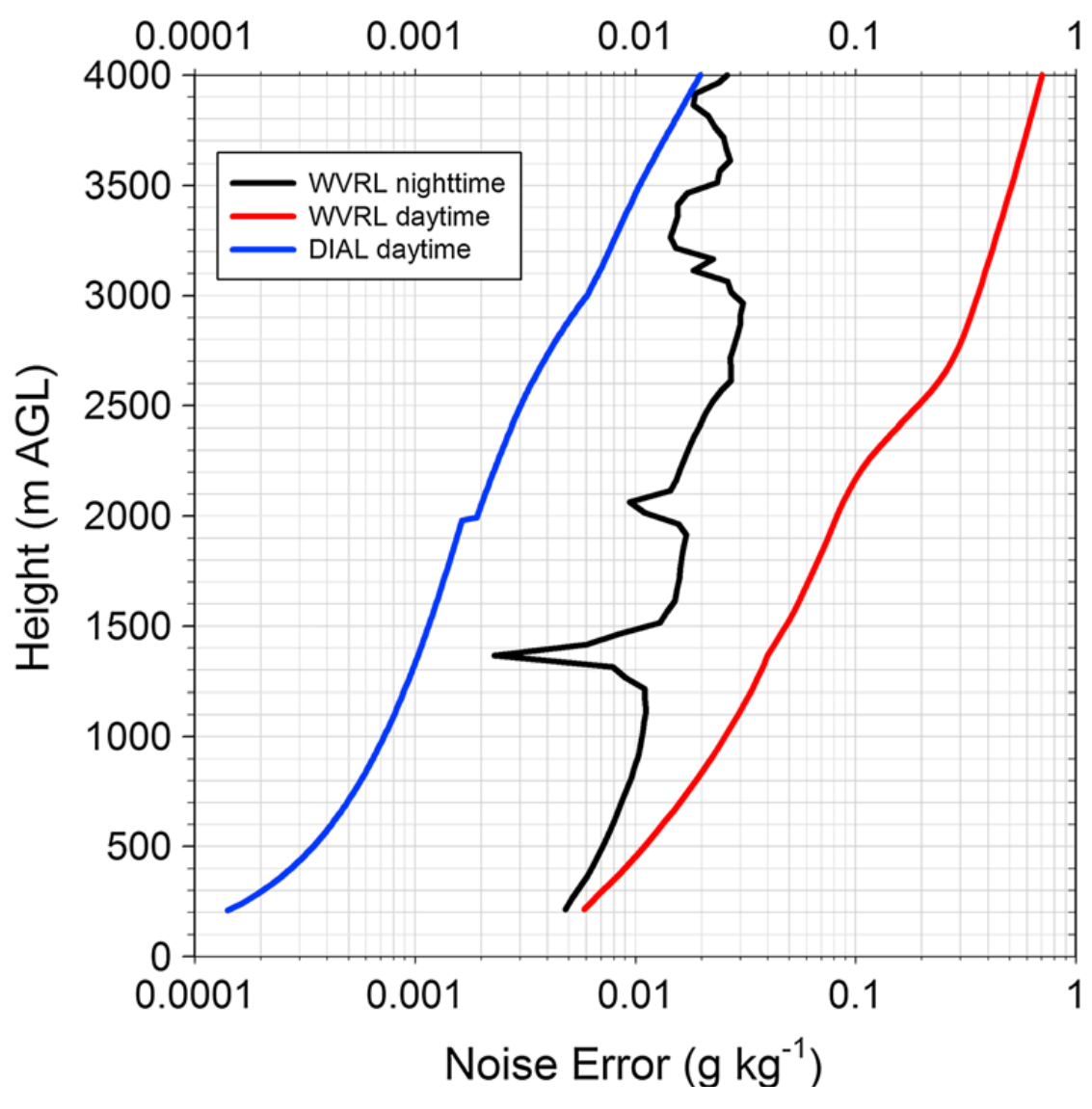
This results in a stronger noise averaging behavior with respect to the range resolution in comparison to Raman lidar because the relative error is also dependent on the differential optical thickness in the range cell $\Delta \tau_{WV}$.

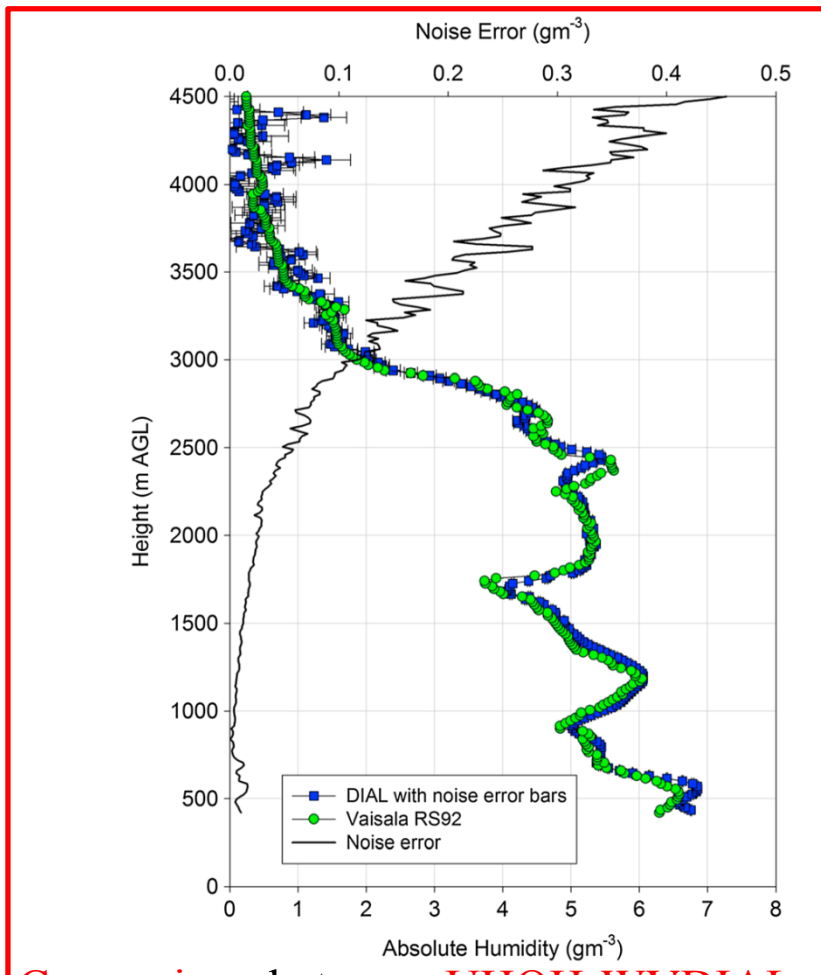


An increased range resolution translates into a strongly increased measurement uncertainty.

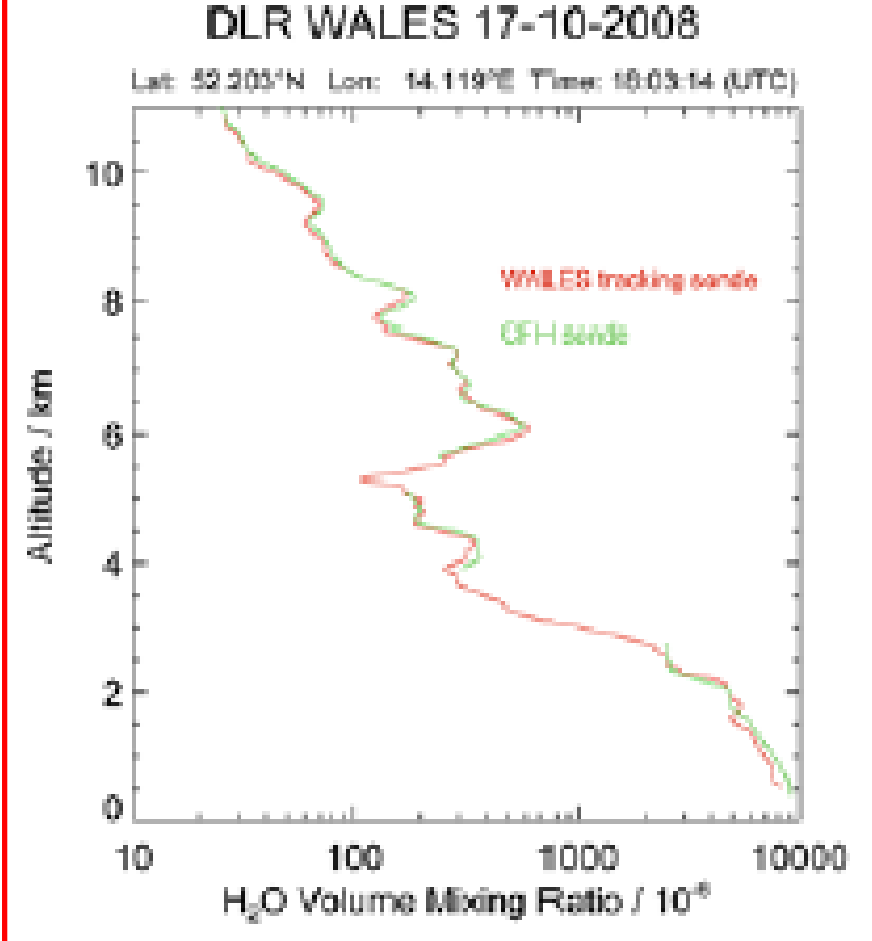
Uncertainty affecting water vapour DIAL measurements

- Noise error simulations of WVRL and WVDIAL using the same WV profile
- Time and vertical resolution of 10 min and 300 m, respectively.
- The average power and telescope diameter of the WVDIAL were set to 2W and 0.4 m, respectively, whereas 10W and 0.8m were used for the WVRL.





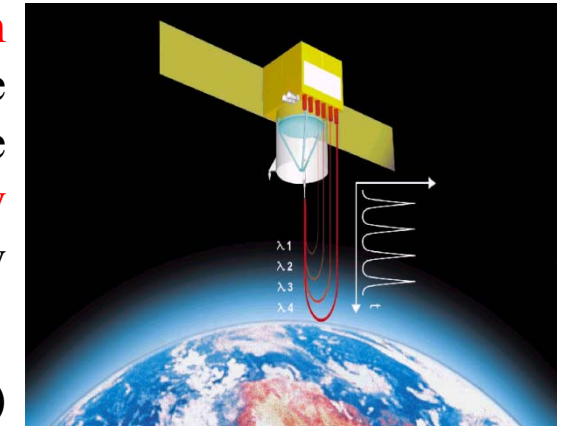
Comparison between UHOH WVDIAL and Vaisala RS92 radiosonde measurements performed on 3 October 2014 at 13:07 UTC. The resolutions of the DIAL profile are 20 min and 150 m, respectively. The noise error of the DIAL profile is also shown.



Comparison between WALES airborne demonstrator, developed by the German Aerospace Center (DLR), and ballon-borne cryogenic frost point hygrometer (CFH).

Resolution: 200 m vertical / 6 km horizontal

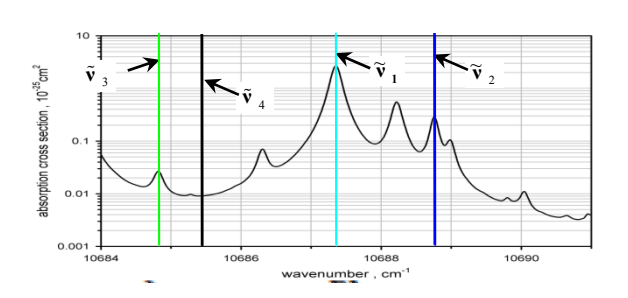
The European Space Agency's Water Vapour Lidar Experiment in Space (WALES) mission (Ehret et al., 2001) was conceived in the frame of the Earth Observation Envelope Programme 2 for the purpose of providing high-quality water vapour profiles, globally and with good vertical resolution, using a DIAL system on a low Earth orbit satellite

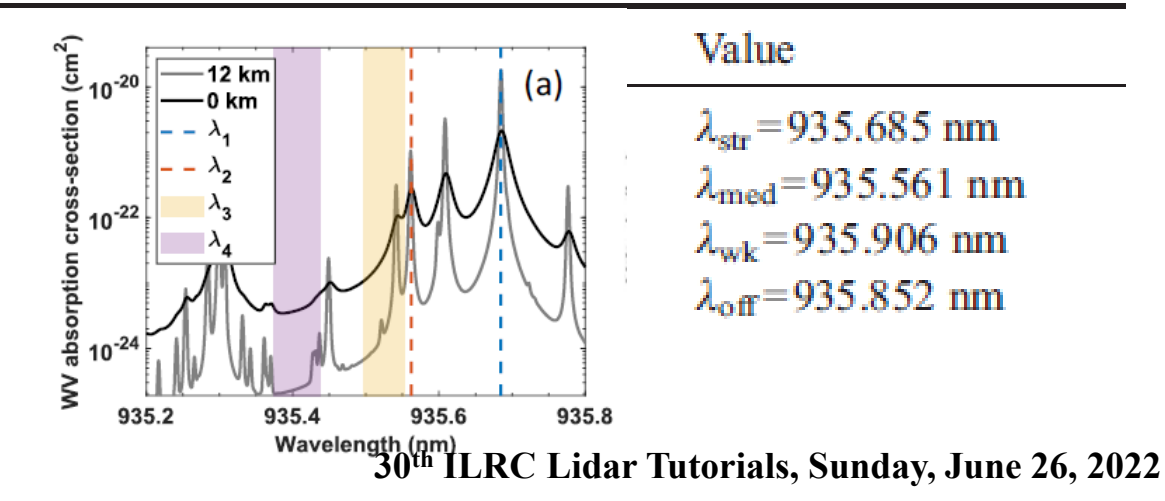


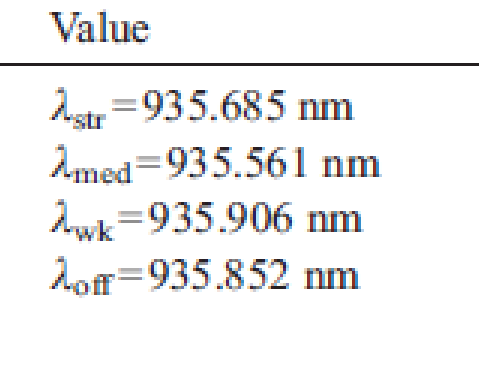
- WALES was finally not selected for the design phase (phase B) based primarily on cost estimates and because of development risks identified in the DIAL transmitter.
- A large water vapor dynamics can be covered only if several absorption lines are selected and simultaneously used.
- In this regard the tricky approach considered in the WALES experiment and implemented in the WALES airborne demonstrator (DLR) and in HALO (NASA) was using 4 different wavelengths forming 3 different online-offline wavelength pairs.

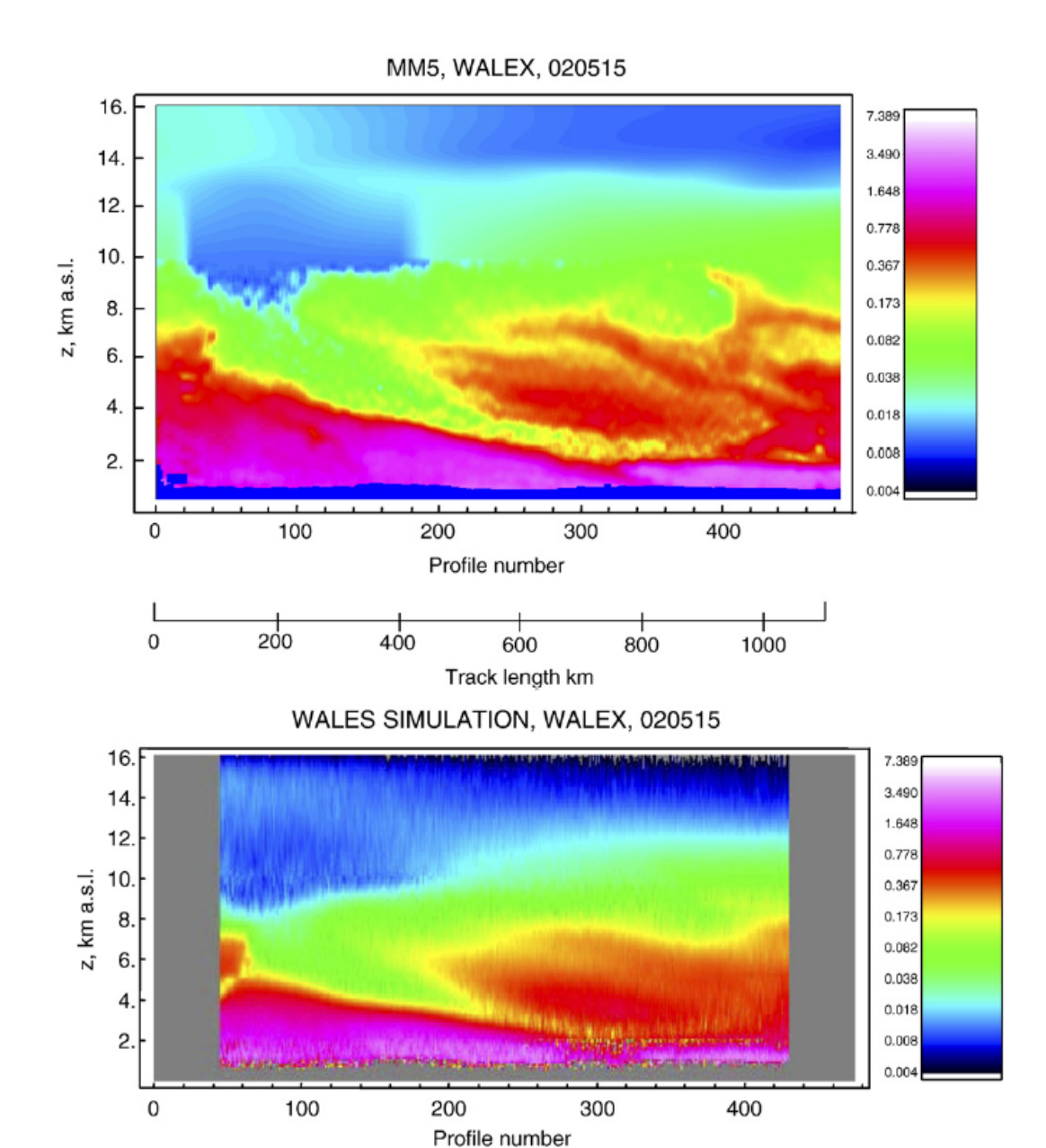
Parameter

Laser wavelengths









Space DIAL reconstruction of theWALEX humidity field (horizontal resolution of 25 km up to the PBL top, of 100 up to 5 km, of 150 up to 10 km and of 200 above 10 km).

